RSC Advances

PAPER

View Article Online
View Journal | View Issue

Cite this: *RSC Adv.*, 2019, **9**, 36600

Palladium/phosphorus-functionalized porous organic polymer with tunable surface wettability for water-mediated Suzuki–Miyaura coupling reaction†

Yizhu Lei,*[a] Zaifei Chen[a] and Guangxing Li*[b]

Received 24th August 2019
Accepted 1st November 2019

DOI: 10.1039/c9ra06680b

rsc.li/rsc-advances

A series of phosphorus-functionalized porous organic polymers supported palladium catalysts with tunable surface wettability were successfully prepared using an easy copolymerization and successive immobilization method. The obtained polymers were carefully characterized by many physicochemical methods. Characterization results suggested that the prepared materials featured hierarchically porous structures, high pore volumes, tunable surface wettability and strong electron-donating ability towards palladium species. We demonstrated the use of these solid catalysts for water-mediated Suzuki–Miyaura coupling reactions. It was found that the surface wettability of the prepared catalysts has an important influence on their catalytic activities. The optimal catalyst, which has excellent amphipathicity and relatively high phosphorus concentration, displayed superior catalytic activity compared to the other catalysts. Under ambient conditions, a variety of aryl chlorides can be efficiently transformed to biaryls in high yields. Moreover, the catalyst could be easily recovered and reused at least six times.

Introduction

The increasing environmental concerns about harmful solvent waste has led to a considerable interest of performing organic transformations in water medium.[1,2] As nature's chosen medium, water not only offers the advantages of nontoxicity, nonflammability, ecological friendliness and low price,[1,2] but also accelerates some reactions' rates through the hydrophobic or "on water" effects.[3] On the other hand, heterogeneous switching of homogeneous catalysis is considered as an important strategy for realizing environmentally benign transformations.[4] Therefore, there is good reason to believe that developing highly efficient solid catalysts for the aqueous and heterogeneous switch of homogeneous organic reactions would be an ideal pathway for green and sustainable organic synthesis.

Triphenylphosphine (PPh_3) and its derivatives are one kind of the most important organic ligands that have been widely used in homogeneous transition-metal catalysis.[5] However, the air-sensitivity and thermal instability of phosphorus ligands at high temperature make the recycling/recovery of their metal complexes difficult, and thus, restricting their more extensive applications.[6] Heterogenization of a homogeneous metal complex by immobilizing the metal complex onto a solid support with the covalent bond has been expected to address these problems,[7] where organic polymers[8] and porous silicas[9] are the most widely used catalyst supports. Porous silicas feature high surface area and stable porous structure, however, their inert chemical nature limits their post-surface chemical modification.[10] Conventional polymers feature easy chemical modification, nevertheless, the polymer-anchored molecular catalysts often suffer from poor stability, inhomogeneously distributed active sites, and low efficiency in mass transport.[11]

Porous organic polymers (POPs), which feature high surface areas, and designable chemical structure, have attracted tremendous research interest as new catalyst supports recently due to their potential to combine the best features of homogeneous and heterogeneous catalysts.[12] In recent years, a number of POPs containing PPh_3 ligand and its derivatives, have been successfully prepared and applied as the catalyst supports for immobilizing transition metal complexes.[5b,6,13] Due to the strong interaction between transition metals and phosphine ligands, transition metals supported on phosphine functionalized POPs usually exhibited long-term reusability, excellent leaching resistant ability, and high catalytic activities.[6,13,14] Some of them even outperformed the activities of their homogeneous analogues.[6a,15] However, performing an organic reaction in water over a solid catalyst inevitably suffers from poor mass transfer efficiency of the hydrophobic organic substances, and thus, leading to low catalytic efficiency.[16] To address this

[a]School of Chemistry and Materials Engineering, Liupanshui Normal University, Liupanshui, Guizhou 553004, PR China. E-mail: yzleiabc@126.com
[b]Jingchu University of Technology, Jingmen, Hubei 448000, PR China. E-mail: ligxabc@163.com

† Electronic supplementary information (ESI) available. See DOI: 10.1039/c9ra06680b

problem, surface of the solid catalyst could be designed to be amphiphilic.[17] Nevertheless, the overwhelming majority of POPs, as well as those phosphine functionalized POPs, were mainly composed of hydrophobic aromatic networks. The hydrophobic properties lead to their poor dispersion in water and thus restricted their applications in water.[18]

Catalytic performance of a heterogeneous catalytic process is usually affected by the following two parameters: (i) structure of the active sites, (ii) the adsorption, desorption, and surface transfer of the reactants and products.[19] It is well known that the catalyst wettability plays an important role in manipulation of the adsorption, desorption and surface transfer behaviour of the reactants and products.[20] Therefore, designing heterogeneous catalysts with suitable wettability could improve the catalytic performances.[19–21] Recently, several investigations about the importance of POPs' wettability in catalysis have been reported,[21,22] however, studies of POPs with tunable wettability and their catalytic performances in aqueous-phase catalysis have rarely been explored.

In this study, a series of phosphorus-functionalized porous organic polymers (PTVP-MBA) supported palladium catalysts were successfully prepared by a free-radical cross-linked copolymerization of tris(4-vinylphenyl)phosphine (TVP) and *N*,*N*′-methylenebisacrylamide (MBA), and successive immobilization of palladium species method. By simply varying the MBA/TVP mass ratio, the palladium catalysts with varied surface wettability from hydrophobic to hydrophilic could be systematically obtained. The obtained palladium catalysts were tested in Suzuki–Miyaura coupling reactions between aryl chlorides and arylboronic acids. At room temperature, the optimal catalyst exhibited excellent catalytic performance in water.

Results and discussion

Synthesis and characterization of the catalysts

Porous PTVP-MBA-*x* polymers (*x* refers to the mass ratio of TVP to the total monomers) were directly synthesized through a solvothermal, free-radical copolymerization reaction of TVP and MBA (Scheme 1). For adjusting the wettability of PTVP-MBA-*x* polymers, PTVP-MBA-*x* polymers with different phosphine contents (PTVP-MBA-*x*, $x = 0.2, 0.3, 0.4, 0.5, 0.6, 0.8$) were synthesized by varying the mass ratio of tris(4-vinylphenyl) phosphine monomer. For comparison, TVP homopolymer (POL-PPh_3, $x = 1.0$) was also synthesized.

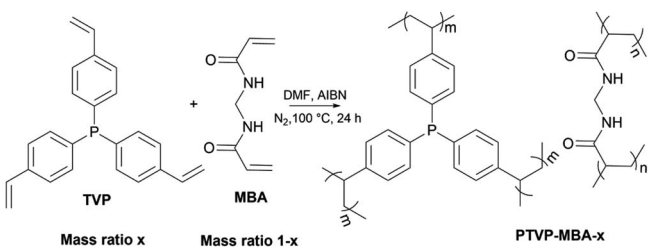

Scheme 1 Synthetic scheme for the PTVP-MBA-*x* polymers.

The porous properties of PTVP-MBA-*x* and POL-PPh_3 were measured by nitrogen adsorption–desorption isotherm measurements at 77 K. As shown in Fig. 1, all the samples displayed the combined features of type I and type IV curves. The two obvious steep steps of nitrogen gas uptake in the $P/P_0 < 0.01$ and $0.80 < P/P_0 < 1.0$ regions indicated the presence of micropores and macropores, while the hysteresis loops at P/P_0 in the range of 0.7–1.0 reflected the presence of mesopores. Consistently, pore size distribution curves (inset) based on the NLDFT calculation method also confirmed the presence of hierarchically porous structure. Such a hierarchical pore structure has been found to be beneficial for heterogeneous catalysts by accelerating the mass transport of reactants and products.[23] Specific surface areas and total pore volumes of the samples were also listed in Table 1. The results indicated that BET surface areas of the samples decreased from 1146 $m^2\ g^{-1}$ to 647 $m^2\ g^{-1}$ with the mass ratio (*x*) of TVP varied from 1.0 to 0.5. Further decreasing the mass ratio (*x*) of TVP below 0.5, BET surface areas of the samples (PTVP-MBA-*x*, $x = 0.4, 0.3, 0.2$) maintained at about 650 $m^2\ g^{-1}$. Meanwhile, with TVP mass ratio (*x*) varied from 1.0 to 0.2, total pore volumes of the samples decreased previously from a maximum value (2.41 $cm^3\ g^{-1}$, POL-PPh_3) to a minimum value (0.93 $cm^3\ g^{-1}$, $x = 0.6$) and then increased later to a moderate value (1.68 $cm^3\ g^{-1}$, $x = 0.2$).

Selected SEM images of three representative samples (PTVP-MBA-*x*, $x = 0.2, 0.4, 0.6$) were shown in Fig. 2A–C. These images showed that the copolymers had the similar sponge-like morphologies, which consisted of loosely packed and

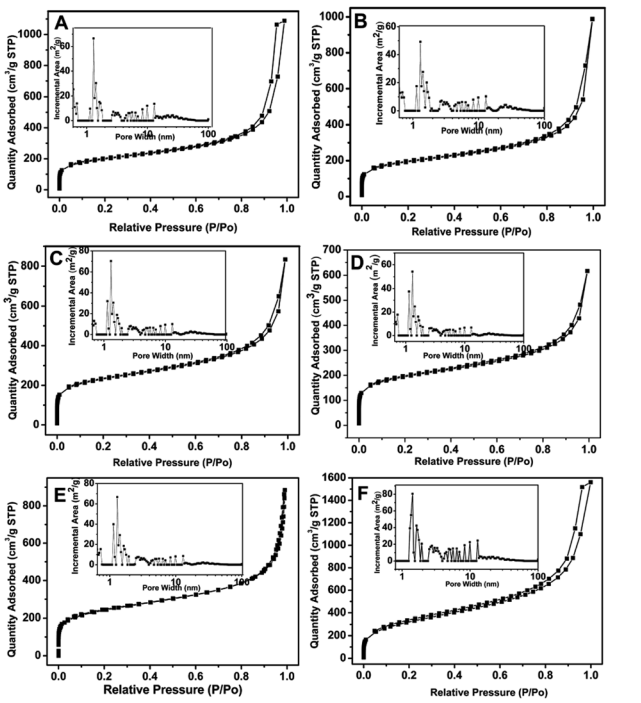

Fig. 1 N_2 absorption–desorption isotherms and pore size distribution curves (inset) of PTVP-MBA-*x* samples at 77 K. (A) PTVP-MBA-0.2, (B) PTVP-MBA-0.3, (C) PTVP-MBA-0.4, (D) PTVP-MBA-0.5, (E) PTVP-MBA-0.6, (F) PTVP-MBA-0.8.

Table 1 Textural properties

Samples	S_{BET}[a] ($m^2\ g^{-1}$)	V_p[b] ($cm^3\ g^{-1}$)	D_{ave}[c] (nm)
PTVP-MBA-0.2	663	1.68	10.2
PTVP-MBA-0.3	646	1.53	9.4
PTVP-MBA-0.4	675	1.29	6.7
PTVP-MBA-0.5	647	0.95	5.9
PTVP-MBA-0.6	760	0.93	4.9
PTVP-MBA-0.8	834	1.36	6.5
POL-PPh_3	1146	2.41	8.4

[a] BET surface area. [b] Total pore volume. [c] Average pore size.

irregular-shape nanoparticles. SEM image of Pd^{II}@PTVP-MBA-0.4 in Fig. 2D showed that the sponge-like morphology remained unchanged after coordination with $Pd(OAc)_2$. TEM image of PTVP-MBA-0.4 in Fig. S1 (ESI†) further confirmed the loosely packed and sponge-like morphology.

Fig. 3 showed the FT-IR spectra of the monomers and representative polymers. Peaks at 2930 and 2859 cm^{-1} in associated with the stretching vibration of $-CH_2$ and –CH groups could be clearly observed for all PTVP-MBA-*x* samples. Peaks at 1661 cm^{-1} assigned to the C=O bond of amide group, were also clearly observed for PTVP-MBA-*x* samples, indicating the presence of the MBA component. Peaks at 825 cm^{-1} were related to C–H out-plane flexural vibration of 1,4-substituted benzene ring, indicating the successful introduction of the TVP component. Additionally, Fig. 3a and b showed a stretching vibration band of terminal vinyl group at around 1627 cm^{-1}, and this band was disappeared after polymerization reaction, revealing that the polymerization reactions were finished.

To gain insight into the structural information and coordination states of Pd species, XPS studies have been performed on the PTVP-MBA-0.4 support and three representative Pd^{II}@PTVP-MBA-*x* ($x = 0.2, 0.4, 0.6$) catalysts. In Fig. S2,† XPS full spectra of PTVP-MBA-0.4 and Pd^{II}@P(TSP-MBA)-0.4 validated that C, N, P and O elements were present in the porous polymer and

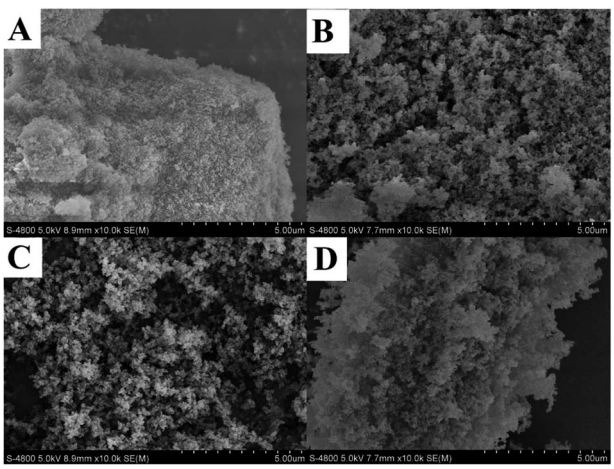

Fig. 2 SEM images for: (A) PTVP-MBA-0.2; (B) PTVP-MBA-0.4; (C) PTVP-MBA-0.6 and (D) Pd^{II}@PTVP-MBA-0.4.

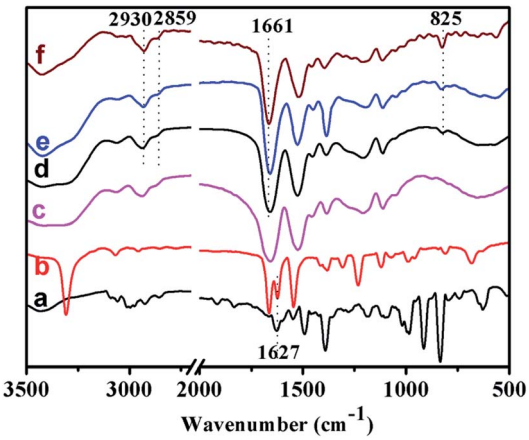

Fig. 3 FT-IR spectra of the monomers and polymers: (a) TVP, (b) MBA, (c) POL-PPh_3, (d) PTVP-MBA-0.2, (e) PTVP-MBA-0.4, and (f) PTVP-MBA-0.6.

catalysts. As depicted in Fig. 4A, Pd 3d XPS spectra of Pd^{II}@PTVP-MBA-*x* ($x = 0.2, 0.4, 0.6$) samples revealed that Pd species were present in the Pd(II) state. The binding energies of Pd $3d_{5/2}$ were around 337.4 eV for Pd^{II}@PTVP-MBA-*x* ($x = 0.2$, 0.4, 0.6) samples. These values are lower than that (338.4 eV) of free $Pd(OAc)_2$.[24] Simultaneously, the P 2p binding energies of Pd^{II}@PTVP-MBA-*x* ($x = 0.2, 0.4, 0.6$) samples exhibited higher values than that (132.0 eV) of PTVP-MBA-0.4. These results suggested that there was a strong coordination interaction between Pd species and PPh_3 ligand in the frameworks. ICP-AES results (Table S1, ESI†) showed that the palladium contents in Pd^{II}@PTVP-MBA-*x* ($x = 0.2, 0.3, 0.4, 0.5, 0.6, 0.8$) and Pd^{II}@POL-PPh_3 catalysts were very close to the nominal amount (2 wt%), suggesting the excellent palladium immobilization abilities of the prepared polymers. In the following catalytic experiments, nominal palladium content (2 wt%) was used for Pd^{II}@PTVP-MBA-*x* ($x = 0.2, 0.3, 0.4, 0.5, 0.6, 0.8$) and Pd^{II}@POL-PPh_3 catalysts. Elemental components of the PTVP-MBA-*x* ($x = 0.2$, 0.3, 0.4, 0.5, 0.6, 0.8) samples were also examined by elemental analysis (Table S2, ESI†). The results suggested that the C, H, O, N, and P contents of the samples were very close to theoretical values, with relative deviation lower than 5%. To study the element dispersion of Pd^{II}@PTVP-MBA-*x*, SEM-mapping of

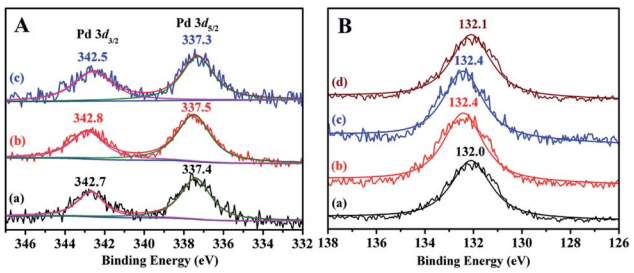

Fig. 4 (A) Pd 3d XPS spectra of Pd^{II}@PTVP-MBA-0.2 (a), Pd^{II}@PTVP-MBA-0.4 (b) and Pd^{II}@PTVP-MBA-0.6 (c); (B) P 2p XPS spectra of PTVP-MBA-0.4 (a), Pd^{II}@PTVP-MBA-0.2 (b), Pd^{II}@PTVP-MBA-0.4 (c) and Pd^{II}@PTVP-MBA-0.6 (d).

Pd^{II}@PTVP-MBA-0.4 was examined (Fig. S3, ESI†). Obviously, C, N, O, P, and Pd elements were well distributed with high degrees of dispersion. Thermogravimetric analyses (TGA) of PTVP-MBA-x (x = 0.2, 0.4, 0.6) samples (Fig. S4, ESI†) showed that the main weight loss occurred above 300 °C, suggesting that the prepared samples could be stable up to 300 °C. A little weight loss around 4 wt% could be also observed bellow 100 °C; this weight loss could be mainly ascribed to the removal of trapped guest molecules, which is common for porous materials.

The solid-state ^{13}C CP/MAS spectra of PTVP-MBA-0.4 and Pd^{II}@PTVP-MBA-0.4 were almost identical (Fig. S5, ESI†). The bands at about 175 ppm were assignable to "C=O" carbon. The bands ranged from 126 to 149 ppm could be attributed to the aromatic carbons of the samples.[13b] While the bands ranged from 30 to 43 ppm could be ascribed to the polymerized vinyl groups.[15a] These results provided additional evidence for the successful synthesis of the copolymer. The solid state ^{31}P CP/MAS spectra of PTVP-MBA-0.4 and Pd^{II}@PTVP-MBA-0.4 were shown in Fig. S6 (ESI†). The ^{31}P CP/MAS spectrum of PTVP-MBA-0.4 displayed a main peak at 5.80 ppm and a small peak at 27.52 ppm. The peak at −5.80 ppm could be attributed to phosphorus in a tertiary state.[13b,e] While the peak at 27.52 ppm was assignable to the oxidation state of phosphorus (P=O),[13e] indicating partial oxidation of tertiary phosphorus occurred during the polymerization reaction. The ^{31}P CP/MAS spectrum of Pd^{II}@PTVP-MBA-0.4 displayed two peaks at −6.36 ppm and 28.31 ppm. The peak at −6.36 ppm was assignable to the uncoordinated tertiary phosphorus; while the peak at 28.31 ppm could be ascribed to both the phosphorus atoms coordination with palladium and the oxidation state of phosphorus (P=O).[13e] This downfield shift of the resonance peak confirmed the electron-donating character of phosphine ligands. This result was consistent with XPS analyses.

Wettability control of the solid catalyst is an important and efficient strategy towards high catalytic performance, especially for organic transformations in water.[18] The MBA monomer is hydrophilic, while TVP is hydrophobic. Therefore, PTVP-MBA-x samples with different content of MBA should exhibit different wettability properties. To test surface wettability of the obtained catalysts, the water contact angle measurement was conducted. As shown in Fig. 5 and S7,† Pd^{II}@POL-PPh_3 had the contact angle of nearly 113°, indicating its water-repellent property. With increasement of the content of MBA, the water contact angles for the samples gradually decreased. Pd^{II}@PTVP-MBA-0.8 and Pd^{II}@PTVP-MBA-0.6 had the contact angles of 59° and 16° for water droplets, respectively. When the mass ratio of MBA in the sample was no less than 0.5, the water droplets were totally absorbed by the porous samples without any residue. Thus, the water contact angles of Pd^{II}@PTVP-MBA-x (x = 0.2, 0.3, 0.4, 0.5) were recorded as 0°. These superhydrophilic features should be related to their hydrophilic and porous structures. Contact angle measurements between toluene and Pd^{II}@PTVP-MBA-x were also conducted to test their lipophilicity. The results showed that toluene drops were totally absorbed without any residue for all the Pd^{II}@PTVP-MBA-x and Pd^{II}@POL-PPh_3 catalysts. Thus, this copolymerization strategy provides an efficient method for synthesizing amphiphilic catalysts that enables the flexible tuning of their water-wettability at a molecular level.

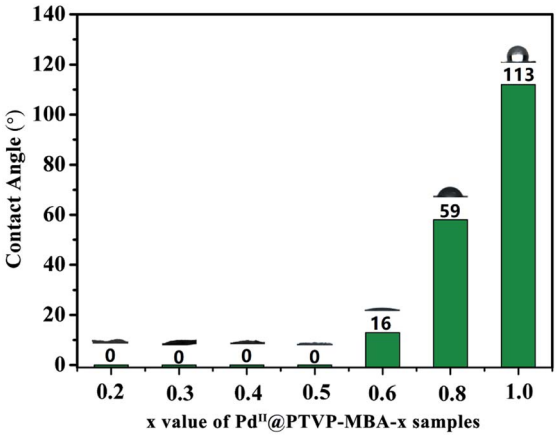

Fig. 5 Contact angle measurements of the prepared catalysts for water.

Suzuki–Miyaura coupling reactions of aryl chlorides

With the expected materials in hand, Suzuki–Miyaura coupling of aryl halides, which is a typical coupling reaction, was employed to investigate the catalytic performance of the obtained palladium catalysts.[4c,5b,6a,13e] To optimize the reaction conditions, coupling reaction of phenylboronic acid with chlorobenzene was adopted for initial studies (Table 2). First the reaction was conducted with Pd^{II}@PTVP-MBA-0.5 as a catalyst to screen the bases (entries 1–7). Under the described conditions at 25 °C, K_2CO_3 afforded the best catalytic performance, and a 75% yield of biphenyl was gained in 8 h (entry 2). Then, catalytic activities of the obtained Pd^{II}@PTVP-MBA-x were tested. Interestingly, catalytic activities of Pd^{II}@PTVP-MBA-x catalysts changed obviously with the mass ratio (x) of TVP varied from 0.8 to 0.2, and reaching a maximum yield (83%) with Pd^{II}@PTVP-MBA-0.4 as a catalyst (entries 9–13). Examination of entry 14 and 15 showed that no homocoupling product was obtained in the absence of chlorobenzene or phenylboronic acid, suggesting that homocoupling reaction of phenylboronic acid or chlorobenzene couldn't occur under the reaction conditions. Thus, the significant difference in yields over different Pd^{II}@PTVP-MBA-x catalysts should be mainly attributed to their difference in the surface wettability. Pd^{II}@POL-PPh_3, which had the highest PPh_3 density, however, gave the lowest yield of biphenyl (entry 8). This low catalytic performance could be attributed to its hydrophobic property, which led to its poor dispersion in water and low accessibility to the reactants. With mass ratio of hydrophobic TVP decreased from 1.0 to 0.4, the surface wettability changed from hydrophobic to hydrophilic, and the yields of biphenyl were significantly increased. However, further decreasing the x from 0.4 to 0.2, the yields were decreased. This decrease could be attributed to the low PPh_3 concentrations in the PTVP-MBA-0.2 and PTVP-MBA-0.3

Table 2 Effects of catalysts and bases on the Suzuki–Miyaura coupling of chlorobenzene and phenylboronic acid[a]

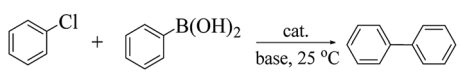

Entry	Catalyst	Base	T (h)	Yield[b] (mol%)
1	Pd^{II}@PTVP-MBA-0.5	Na_2CO_3	8	71
2	Pd^{II}@PTVP-MBA-0.5	K_2CO_3	8	75
3	Pd^{II}@PTVP-MBA-0.5	K_3PO_4	8	55
4	Pd^{II}@PTVP-MBA-0.5	DBU	8	21
5	Pd^{II}@PTVP-MBA-0.5	Et_3N	8	14
6	Pd^{II}@PTVP-MBA-0.5	NaOH	8	23
7	Pd^{II}@PTVP-MBA-0.5	$NaHCO_3$	8	11
8	Pd^{II}@POL-PPh_3	K_2CO_3	8	12
9	Pd^{II}@PTVP-MBA-0.8	K_2CO_3	8	29
10	Pd^{II}@PTVP-MBA-0.6	K_2CO_3	8	57
11	Pd^{II}@PTVP-MBA-0.4	K_2CO_3	8	88
12	Pd^{II}@PTVP-MBA-0.3	K_2CO_3	8	81
13	Pd^{II}@PTVP-MBA-0.2	K_2CO_3	8	72
14[c]	Pd^{II}@PTVP-MBA-0.4	K_2CO_3	8	—
15[d]	Pd^{II}@PTVP-MBA-0.4	K_2CO_3	8	—
16	Pd/C	K_2CO_3	15	—
17[e]	Pd/C	K_2CO_3	15	21
18	$PdCl_2(PPh_3)_2$	K_2CO_3	12	<3
19	Pd^{II}@PTVP-MBA-0.4	K_2CO_3	12	98
20[f]	Pd^{II}@PTVP-MBA-0.4	K_2CO_3	12	82

[a] Reaction conditions: Pd 1.0 mol%, chlorobenzene 1.0 mmol, phenylboronic acid 1.5 mmol, base 2.0 mmol, water 3 mL, 25 °C, 1000 rpm. [b] GC yields. [c] Without chlorobenzene. [d] Without phenylboronic acid. [e] PPh_3 2.0 mol%. [f] Pd 0.5 mol%.

Table 3 Suzuki–Miyaura coupling of aryl chlorides and arylboronic acids catalyzed by Pd^{II}@PTVP-MBA-0.4[a]

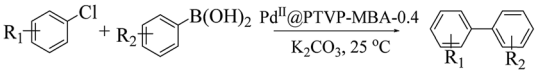

Entry	R^1	R^2	Time (h)	Yield[b] (mol%)
1	4-CH_3	H	12	93
2	4-OCH_3	H	14	94
3	4-NH_2	H	15	87
4	4-OH	H	10	99
5	4-$COCH_3$	H	12	96
6	4-F	H	12	96
7	4-Ph	H	16	81
8	4-NO_2	H	12	97
9	3-NO_2	H	12	92
10	2-NO_2	H	24	78
11	2-NO_2	H	10	98[c]
12	4-OCH_3	4-CH_3	12	92
13	4-OCH_3	4-C_2H_5	12	97
14	4-OCH_3	4-CF_3	12	91
15	4-OCH_3	4-CN	12	95
16	4-CH_3	4-CH_3	12	94
17	4-CHO	4-CHO	11	95

[a] Reaction conditions: Pd^{II}@PTVP-MBA-0.4 (Pd 1.0 mol%), aryl chlorides 1.0 mmol, arylboronic acids 1.5 mmol, K_2CO_3 2.0 mmol, water 3 mL, 25 °C, 1000 rpm. [b] Isolated yields. [c] Reaction temperature 50 °C.

networks. The importance of PPh_3 ligand was further ascertained by the catalytic performance of Pd/C under the optimal conditions. Pd/C gave no target product, while a 21% yield was gained in the presence of 2.0 mol% PPh_3 (entries 16 and 17). For comparison, $PdCl_2(PPh_3)_2$, a traditional homogeneous catalyst for this coupling reaction, was also tested. However, $PdCl_2(PPh_3)_2$ gave the target product in trace yield (entry 18); this could be attributed to the poor hydrophilicity and quick formation of palladium black of $PdCl_2(PPh_3)_2$. The effects of reaction time and catalyst usage were also investigated (entries 19 and 20), and a 98% yield of biphenyl was obtained at 12 h with 1 mol% of Pd^{II}@PTVP-MBA-0.4. Thus, an efficient and water-compatible catalyst was obtained with fine-turning the composition of the polymer support.

To investigate the scope of Pd^{II}@PTVP-MBA-0.4 catalyst in Suzuki–Miyaura coupling reaction, aryl chlorides and arylboronic acids bearing different functional groups were tested (Table 3). The results showed that aryl chlorides bearing electron-donating groups such as methyl, methoxy, and amino, gave the biaryls as the sole product in high yields (entries 1–3), but longer reaction times were needed for the latter two substrates. This slower rate of reaction might be due to the strong electron-donating effect of the substituent groups, which resulted in stronger strength of C–Cl bond and lower rate of oxidative addition step.[25] Conversely, 4-chlorophenol, although bearing an electron-donating hydroxy group, gave the corresponding biaryl in 99% after only 10 h. This higher reaction rate might be due to the good solubility of 4-chlorophenol in water. Under ambient conditions, aryl chlorides bearing electron-withdrawing groups at the *para* position also participated in the reactions readily, affording the corresponding biaryls in moderate to excellent yields within 16 h (entries 5–8). Sterically hindered substrates such as 3-nitrochlorobenzene and 2-nitrochlorobenzene also gave good yields of biaryls, but a prolonged reaction time or elevated reaction temperature was needed (entries 9–11). The same protocol was also successfully extended to several *para*-substituted arylboronic acids, and high yields of desired biaryls were obtained (entries 12–15). Symmetrical biaryls, 4,4′-dimethyl and 4,4′-dicarbaldehyde biphenyls, could be gained in high yields (entries 16 and 17). Rather surprisingly, although most of aryl chlorides in Table 3 are either solids or poorly soluble in water, good yields of biaryls could be gained despite the fact that dissolution could limit reaction efficiency. Thus, this study offers an active and heterogeneous catalyst for the Suzuki–Miyaura coupling of aryl chlorides and arylboronic acids in water.

In addition to catalytic activity, reusability and metal leaching of the catalyst are also important factors in the heterogeneous catalytic systems for commercial applications. The reaction of chlorobenzene with phenylboronic acid was selected to evaluate the recycling capacity of Pd^{II}@PTVP-MBA-0.4. After each cycle, the yield of desired biaryl was analysed by GC, and the Pd content in the filtrate was analysed by ICP-AES. As shown

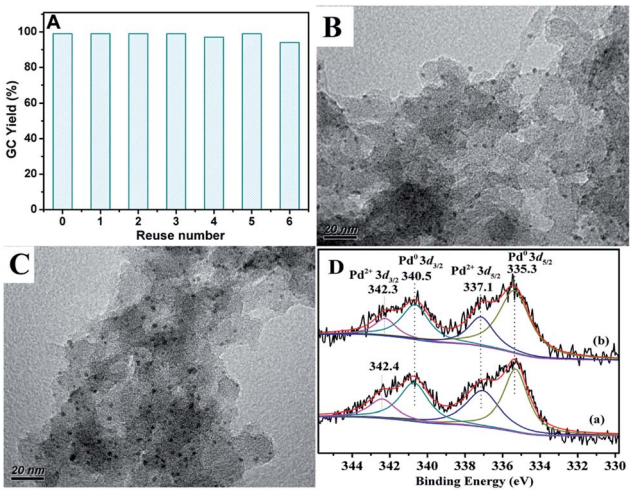

Fig. 6 (A) Reuse of the Pd^{II}@PTVP-MBA-0.4 for the Suzuki cross-couplings of chlorobenzene with phenylboronic acid. The reaction conditions were the same with that of entry 19 in Table 2; (B) TEM image for the recycling Pd^{II}@PTVP-MBA-0.4 after the first run; (C) TEM image for the recovered Pd^{II}@PTVP-MBA-0.4 after the 6th recycle; (D) Pd 3d XPS spectra of recycling Pd^{II}@PTVP-MBA-0.4: (a) after the first catalytic run, (b) after the 6th recycle.

in Fig. 6A, Pd^{II}@PTVP-MBA-0.4 exhibited excellent reusability and could be effectively reused at least six times. Moreover, the Pd leaching in the filtrate was undetectable (<10 ppb). The morphology and composition of the recovered catalyst was studied by TEM and XPS. Fig. 6B showed that the Pd nanoparticles with a mean diameter of about 2.5 nm were observed after the first catalytic run (reuse number, 0). Interestingly, no obvious aggregation of Pd nanoparticles occurred up to the 6th recycle (Fig. 6C). Fig. 6D showed that Pd(0) and Pd(II) species coexisted in the recovered catalyst. For the recovered catalyst after reusing 0 and 6 times, the ratios of Pd^0/Pd^{II} were 1.7 and 2.1, respectively (estimated by the proportion of relative peak areas). To investigate further the activity of the recovered catalyst, reaction kinetics were also studied over the catalyst recovered in the 2nd and 6th recycle. As shown in Fig. 7, the yields of biphenyl in the 2nd and 6th recycle were similar to those of the fresh Pd^{II}@PTVP-MBA-0.4 catalyst. These results suggest that the *in situ* formed palladium nanoparticles during the recycles are also highly active for Suzuki–Miyaura coupling reaction, and the catalyst could be recycled at least 6 times without significant loss of activity.

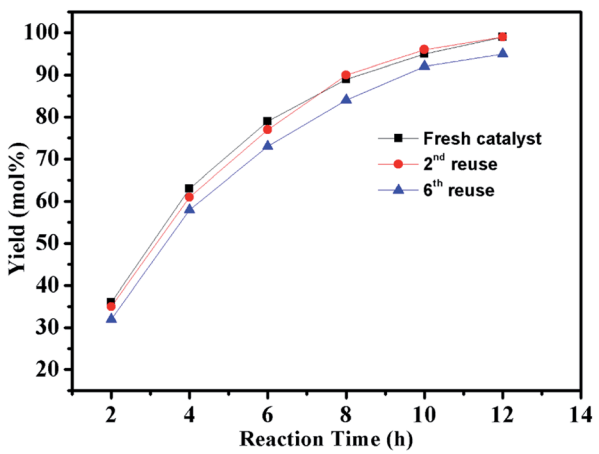

Fig. 7 Reaction kinetics of the catalyst.

Conclusions

In conclusion, porous organic polymers supported palladium catalysts with tunable surface wettability were successfully prepared *via* an easy copolymerization and successive immobilization method. The activity test in aqueous Suzuki–Miyaura coupling reaction suggested that both the surface wettability and phosphorus concentration of the catalyst have important influence on the catalytic activity. The catalyst, which featured excellent amphipathicity and relatively high phosphorus concentration, displayed the highest catalytic activity for water-mediated Suzuki–Miyaura coupling of aryl chlorides. At ambient conditions, a variety of aryl chlorides can be efficiently transformed to biaryls in high yields. Additionally, the catalyst can be easily recovered and reused several times without significant loss of catalytic activity. Thus, this protocol not only provides an efficient heterogeneous catalyst for Suzuki–Miyaura coupling reaction, but also some clues to prepare highly efficient heterogeneous catalysts for aqueous organic reactions.

Experimental

Materials

N,*N*′-Methylenebisacrylamide (99%) and palladium diacetate (99%) were purchased from Energy Chemical and used as received. 2,2′-Azobis(2-methylpropionitrile) (AIBN) was got from Aladdin Chemistry Co., Ltd. (Shanghai, China). Tris(4-vinylphenyl)phosphine was prepared according to our previous report.[6d] Aryl chlorides and arylboronic acids were purchased from commercial suppliers and used without further purification.

Synthesis of PTVP-MBA

Porous PTVP-MBA-*x* polymers (PTVP-MBA-*x*), where *x* refers to the mass ratio of TVP to total monomers, were prepared by a hydrothermal and free-radical cross-linked copolymerization route, at 100 °C for 24 h using dimethylformamide (DMF) as the solvent and AIBN as the initiator. As a typical run, TVP (0.8 g), MBA (1.2 g), DMF (20 mL) and AIBN (0.25 wt%, 50 mg) were added into in a 100 mL Teflon autoclave. After replacement of the air in the autoclave with nitrogen, stirred at room temperature for 2 h, the autoclave was heated statically in an oven at 100 °C for 24 h. After cooling to room temperature, the resulting monolith solid was extracted with ethanol and dried under vacuum (60 °C). The obtained white polymer was designated as PTVP-MBA-0.4. Varying the mass ratio of TVP and keeping the same total mass (2.0 g) of two monomers, other PTVP-MBA-*x*

polymers were prepared as the same synthetic procedures of PTVP-MBA-0.4.

Synthesis of Pd^{II}@PTVP-MBA-*x*

To prepare 2.0 wt% Pd^{II}@PTVP-MBA-*x*, 42.6 mg of $Pd(OAc)_2$ was first dissolved in 50 mL of acetone, then 1.0 g of PTVP-MBA-*x* was added to the solution. The mixture was stirred at room temperature for 24 h. The resultant solid was separated by centrifugation, washed with acetone for three times, and followed by a Soxlet-extraction for 24 h with acetone. The obtained solid was dried under vacuum (60 °C) for 12 h to give Pd^{II}@PTVP-MBA-*x* as a light-yellow powder.

Synthesis of POL-PPh_3 and Pd^{II}@POL-PPh_3

TVP homopolymer (POP-PPh_3) was synthesized by the reported method.[13b] Pd^{II}@POL-PPh_3 was prepared *via* the same procedures as Pd^{II}@PTVP-MBA-0.4.

Suzuki–Miyaura cross coupling reaction

The catalytic reaction was performed in a 10 mL reaction tube. Generally, Pd^{II}@PTVP-MBA-*x* (53.2 mg, 1.0 mol% Pd) was added to a mixture of arylboronic acid (1.5 mmol), aryl chloride (1.0 mmol) and base (2.0 mmol) in deionized water (3.0 mL). After stirring at 25 °C for the appropriate time, the reaction mixture was treated with ethyl acetate (4 × 5 mL). The catalyst was filtered and washed with ethyl acetate, and the organic fractions combined, dried over anhydrous $MgSO_4$. For the model reaction, the obtained liquid was analyzed by flame ionization (FID) gas chromatography using *N*,*N*-dimethylacetamide as an internal standard. For the investigation of substrate scope, the combined liquid was concentrated under reduced pressure, and the residues were purified by thin-layer chromatography (TLC) using petroleum ether as eluting solvent. Purity of products was checked by ^{1}H NMR and yields were based on aryl chlorides. For the recycling tests of the catalyst, the recovered catalyst was washed with methanol and ethyl acetate, dried under vacuum at 40 °C for 6 h, and then reused in a new catalytic recycle.

Conflicts of interest

There are no conflicts to declare.

Acknowledgements

We acknowledge the financial support by the National Natural Science Foundation of China (21763017); the Science and Technology Fund Project of Guizhou Province (qian ke he ji chu [2018]1414 and [2016]1133); the Scientific and Technological Innovation Platform of Liupanshui (52020-2018-03-02 and 52020-2017-02-02); the Academician Workstation of Liupanshui Normal University (qiankehepingtairencai [2019]5604 hao); and the Fund of Liupanshui Normal University (LPSSYZDXK201602).

References

1 (*a*) T. Kitanosono, K. Masuda, P. Xu and S. Kobayashi, *Chem. Rev.*, 2018, **118**, 679–746; (*b*) M. A. Nasseri, S. A. Alavi, M. Kazemnejadi and A. Allahresani, *RSC Adv.*, 2019, **9**, 20749–20759; (*c*) Y. Dong, Y. Q. Chen, J. J. Jv, Y. Li, W. H. Li and Y. B. Dong, *RSC Adv.*, 2019, **9**, 21671–21678.

2 (*a*) R. Breslow, A Fifty-Year Perspective on Chemistry in Water, in *Organic Reactions in Water*, ed. U. M. Lindström, Blackwell, Oxford, UK, 2007, pp. 1–28; (*b*) Z. Chen and H. Ren, The Applications of Water as Reagents in Organic Synthesis, in *Solvents as Reagents in Organic Synthesis*, ed. X.-F. Wu, Wiley-VCH, New York, 2017, pp. 1–44.

3 (*a*) S. Narayan, J. Muldoon, M. G. Finn, V. V. Fokin, H. C. Kolb and K. B. Sharpless, *Angew. Chem., Int. Ed.*, 2005, **44**, 3275–3279; (*b*) A. Chanda and V. V. Fokin, *Chem. Rev.*, 2009, **109**, 725–748.

4 (*a*) H. Xu, J. Gao and D. Jiang, *Nat. Chem.*, 2015, **7**, 905; (*b*) S. Das, P. Heasman, T. Ben and S. Qiu, *Chem. Rev.*, 2016, **117**, 1515–1563; (*c*) C. A. Wang, K. Nie, G. D. Song, Y. W. Li and Y. F. Han, *RSC Adv.*, 2019, **9**, 8239–8245; (*d*) Y. Dong, J. J. Jv, Y. Li, W. H. Li, Y. Q. Chen, Q. Sun, J. P. Ma and Y. B. Dong, *RSC Adv.*, 2019, **9**, 20266–20272.

5 (*a*) J. F. Hartwig, *Organotransition Metal Chemistry: From Bonding to Catalysis*, University Science Books, Sausalito, 2010, pp. 33–41; (*b*) Z. Guan, B. Li, G. Hai, X. Yang, T. Li and B. Tan, *RSC Adv.*, 2014, **4**, 36437–36443.

6 (*a*) B. Li, Z. Guan, W. Wang, X. Yang, J. Hu, B. Tan and T. Li, *Adv. Mater.*, 2012, **24**, 3390–3395; (*b*) Y. Lei, L. Wu, X. Zhang, H. Mei, Y. Gu and G. Li, *J. Mol. Catal. A: Chem.*, 2015, **398**, 164–169; (*c*) Z. Jia, K. Wang, B. Tan and Y. Gu, *Adv. Synth. Catal.*, 2017, **359**, 78–88; (*d*) Y. Wan, F. Song, T. Ye, G. Li, D. Liu and Y. Lei, *Appl. Organomet. Chem.*, 2019, **33**, e4714.

7 (*a*) D. Wang and D. Astruc, *Chem. Rev.*, 2014, **114**, 6949–6985; (*b*) R. Zhong, A. C. Lindhorst, F. J. Groche and F. E. Kühn, *Chem. Rev.*, 2017, **117**, 1970–2058; (*c*) S. Fukuzumi, Y.-M. Lee and W. Nam, *ChemCatChem*, 2018, **10**, 1686–1702.

8 (*a*) M. Gholinejad, M. Afrasi, N. Nikfarjam and C. Nájera, *Appl. Catal., A*, 2018, **563**, 185–195; (*b*) S. Pan, S. Yan, T. Osako and Y. Uozumi, *ACS Sustainable Chem. Eng.*, 2017, **5**, 10722–10734.

9 (*a*) Z. Guan, J. Hu, Y. Gu, H. Zhang, G. Li and T. Li, *Green Chem.*, 2012, **14**, 1964–1970; (*b*) M. Zhang, R. Ettelaie, T. Yan, S. Zhang, F. Cheng, B. P. Binks and H. Yang, *J. Am. Chem. Soc.*, 2017, **139**, 17387–17396.

10 Q. Sun, Z. Dai, X. Meng and F.-S. Xiao, *Chem. Soc. Rev.*, 2015, **44**, 6018–6034.

11 (*a*) C. A. Wang, Z. K. Zhang, T. Yue, Y. L. Sun, L. Wang, W. D. Wang, Y. Zhang, C. Liu and W. Wang, *Chem.–Eur. J.*, 2012, **18**, 6718–6723; (*b*) S. Wang, K. Song, C. Zhang, Y. Shu, T. Li and B. Tan, *J. Mater. Chem. A*, 2017, **5**, 1509–1515.

12 (*a*) R. Dawson, A. I. Cooper and D. J. Adams, *Prog. Polym. Sci.*, 2012, **37**, 530–563; (*b*) Q. Sun, Z. Dai, X. Meng, L. Wang and F. S. Xiao, *ACS Catal.*, 2015, **5**, 4556–4567; (*c*) Y. Xu, S. Jin, H. Xu, A. Nagai and D. Jiang, *Chem. Soc. Rev.*, 2013, **42**,

8012–8031; (*d*) C. A. Wang, Y. F. Han, Y. W. Li, K. Nie, X. L. Cheng and J. P. Zhang, *RSC Adv.*, 2016, **6**, 34866–34871.

13 (*a*) Q. Zhang, S. Zhang and S. Li, *Macromolecules*, 2012, **45**, 2981–2988; (*b*) Q. Sun, M. Jiang, Z. Shen, Y. Jin, S. Pan, L. Wang, X. Meng, W. Chen, Y. Ding, J. Li and F.-S. Xiao, *Chem. Commun.*, 2014, **50**, 11844–11847; (*c*) Z. Yang, B. Yu, H. Zhang, Y. Zhao, Y. Chen, Z. Ma, G. Ji, X. Gao, B. Han and Z. Liu, *ACS Catal.*, 2016, **6**, 1268–1273; (*d*) C. Li, L. Yan, L. Lu, K. Xiong, W. Wang, M. Jiang, J. Liu, X. Song, Z. Zhan, Z. Jiang and Y. Ding, *Green Chem.*, 2016, **18**, 2995–3005; (*e*) Z. Ding, C. Li, J. Chen, J. Zeng, H. Tang, Y. Ding and Z. Zhan, *Adv. Synth. Catal.*, 2017, **359**, 2280–2287; (*f*) T. Iwai, T. Harada, H. Shimada, K. Asano and M. Sawamura, *ACS Catal.*, 2017, **7**, 1681–1692.

14 S. Doherty, J. G. Knight, T. Backhouse, A. Bradford, F. Saunders, R. A. Bourne, T. W. Chamberlain, R. Stones, A. Clayton and K. Lovelock, *Catal. Sci. Technol.*, 2018, **8**, 1454–1467.

15 (*a*) T. V. Khamatnurova, M. Johnson, D. Santana, H. S. Bazzi and D. E. Bergbreiter, *Top. Catal.*, 2014, **57**, 1438–1444; (*b*) Q. Sun, Z. Dai, X. Liu, N. Sheng, F. Deng, X. Meng and F.-S. Xiao, *J. Am. Chem. Soc.*, 2015, **137**, 5204–5209; (*c*) X. Wang, S. Min, S. K. Das, W. Fan, K.-W. Huang and Z. Lai, *J. Catal.*, 2017, **355**, 101–109.

16 (*a*) B. Lai, F. Mei and Y. Gu, *Chem.–Asian J.*, 2018, **13**, 2529–2542; (*b*) J. O. Weston, H. Miyamura, T. Yasukawa, D. Sutarma, C. A. Baker, P. K. Singh, M. Bravo-Sanchez, N. Sano, P. J. Cumpson, Y. Ryabenkova, S. Kobayashi and M. Conte, *Catal. Sci. Technol.*, 2017, **7**, 3985–3998; (*c*) J. Miguélez, H. Miyamura and S. Kobayashi, *Adv. Synth. Catal.*, 2017, **359**, 2897–2900.

17 (*a*) Y. Gu, C. Ogawa, J. Kobayashi, Y. Mori and S. Kobayashi, *Angew. Chem., Int. Ed.*, 2006, **45**, 7217–7220; (*b*) J. Li, P. Huo, J. Zheng, X. Zhou and W. Liu, *RSC Adv.*, 2018, **8**, 24231–24235; (*c*) G. Shen, T. Osako, M. Nagaosa and Y. Uozumi, *J. Org. Chem.*, 2018, **83**, 7380–7387; (*d*) T. M. Yazdely, M. Ghorbanloo and H. Hosseini-Monfared, *New J. Chem.*, 2019, **43**, 11926–11933.

18 (*a*) R. Dawson, A. Laybourn, R. Clowes, Y. Z. Khimyak, D. J. Adams and A. I. Cooper, *Macromolecules*, 2009, **42**, 8809–8816; (*b*) D. Mullangi, S. Nandi, S. Shalini, S. Sreedhala, C. P. Vinod and R. Vaidhyanathan, *Sci. Rep.*, 2015, **5**, 10876; (*c*) Z. Lv, Q. Sun, X. Meng and F. S. Xiao, *J. Mater. Chem. A*, 2013, **1**, 8630–8635; (*d*) E. R. Rangel, E. M. Maya, F. Sánchez, J. G. de La Campa and M. Iglesias, *Green Chem.*, 2015, **17**, 466–473; (*e*) Y. Lei, Y. Wan, G. Li, X.-Y. Zhou, Y. Gu, J. Feng and R. Wang, *Mater. Chem. Front.*, 2017, **1**, 1541–1549; (*f*) Y. Lei, G. Lan, D. Zhu, R. Wang, X.-Y. Zhou and G. Li, *Appl. Organomet. Chem.*, 2018, **32**, e4421.

19 (*a*) S. Navalon, A. Dhakshinamoorthy, M. Alvaro and H. Garcia, *Chem. Rev.*, 2014, **114**, 6179–6212; (*b*) L. Wang and F. S. Xiao, *Sci. China Mater.*, 2018, **61**, 1137–1142; (*c*) Y. Wu, J. Feng, H. Gao, X. Feng and L. Jiang, *Adv. Mater.*, 2019, **31**, 1800718.

20 (*a*) Y.-Z. Chen, G. Cai, Y. Wang, Q. Xu, S.-H. Yu and H.-L. Jiang, *Green Chem.*, 2018, **18**, 1212–1217; (*b*) Q. Sun, M. Chen, B. Aguila, N. Nguyen and S. Ma, *Faraday Discuss.*, 2017, **201**, 317–326; (*c*) X. Chen, P. Qian, T. Zhang, Z. Xu, C. Fang, X. Xu, W. Chen, P. Wu, Y. Shen, S. Li, J. Wu, B. Zheng, W. Zhang and F. Huo, *Chem. Commun.*, 2018, **54**, 3936–3939.

21 (*a*) Y. Zhang, J. Pan, Y. Shen, W. Shi, C. Liu and L. Yu, *ACS Sustainable Chem. Eng.*, 2015, **3**, 871–879; (*b*) G. Huang, Q. Yang, Q. Xu, S.-H. Yu and H.-L. Jiang, *Angew. Chem., Int. Ed.*, 2016, **55**, 7379–7383; (*c*) Q. Sun, H. He, W. Y. Gao, B. Aguila, L. Wojtas, Z. Dai, J. Li, Y.-S. Chen, F.-S. Xiao and S. Ma, *Nat. Commun.*, 2016, **7**, 13300.

22 (*a*) Y. Zhang, J. Pan, Y. Chen, W. Shi, Y. Yan and L. Yu, *Chem. Eng. J.*, 2016, **283**, 956–970; (*b*) J. Wei, L. Zou and J. Li, *New J. Chem.*, 2016, **40**, 4775–4780; (*c*) H. Gao, J. Pan, D. Han, Y. Zhang, W. Shi, J. Zeng, Y. Peng and Y. Yan, *J. Mater. Chem. A*, 2015, **3**, 13507–13518; (*d*) F. Liu, L. Wang, Q. Sun, L. Zhu, X. Meng and F.-S. Xiao, *J. Am. Chem. Soc.*, 2012, **134**, 16948–16950; (*e*) L. Wang, H. Wang, F. Liu, A. Zheng, J. Zhang, Q. Sun, J. P. Lewis, L. Zhu, X. Meng and F.-S. Xiao, *ChemSusChem*, 2014, **7**, 402–406.

23 T. Yokoi and T. Tatsumi, Hierarchically Porous Materials in Catalysis, in *Hierarchically Structured Porous Materials from Nanoscience to Catalysis, Separation, Optics, Energy, Life Science*, ed. B.-L. Su, C. Sanchez and X.-Y. Yang, Wiley-VCH, Weinheim, 2011, pp. 481–515.

24 S. Y. Ding, J. Gao, Q. Wang, Y. Zhang, W. G. Song, C. Y. Su and W. Wang, *J. Am. Chem. Soc.*, 2011, **133**, 19816–19822.

25 (*a*) J. P. Stambuli, R. Kuwano and J. F. Hartwig, *Angew. Chem., Int. Ed.*, 2002, **41**, 4746–4748; (*b*) R. B. Bedford, C. S. Cazin and D. Holder, *Coord. Chem. Rev.*, 2004, **248**, 2283–2321.